Article

Cell Reports

LSD1 Interacts with Zfp516 to Promote UCP1 Transcription and Brown Fat Program

Graphical Abstract

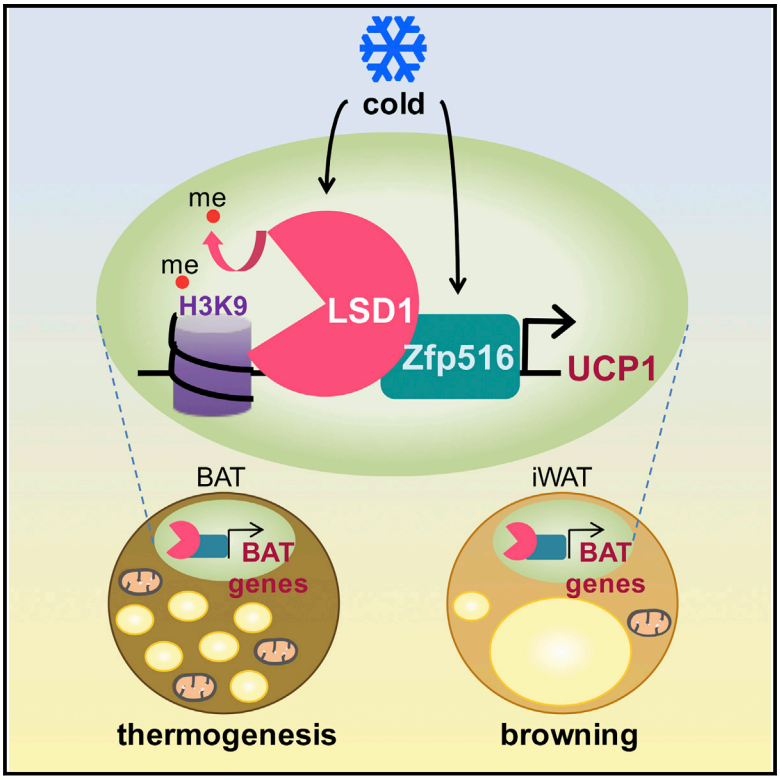

Authors

Audrey Sambeat, Olga Gulyaeva, Jon Dempersmier, Kevin M. Tharp, Andreas Stahl, Sarah M. Paul, Hei Sook Sul

Correspondence

hsul@berkeley.edu

In Brief

Sambeat et al. report that Zfp516, critical for activation of BAT gene program and thermogenesis, directly interacts with LSD1 for recruitment to BAT-enriched thermogenic genes. LSD1 demethylates H3K9 at the promoter regions of BAT-enriched genes. The authors also show that LSD1 is required during embryonic BAT development and for Zfp516-induced browning of WAT.

Highlights

- Zfp516 recruits LSD1 at the UCP1 promoter, where it demethylates H3K9
- LSD1 cooperates with Zfp516 to activate BAT genes and to promote thermogenesis
- LSD1 ablation in brown adipose precursors impairs embryonic development of BAT
- LSD1 ablation prevents browning of subcutaneous WAT induced by Zfp516

Sambeat et al., 2016, Cell Reports *15*, 2536–2549
June 14, 2016
http://dx.doi.org/10.1016/j.celrep.2016.05.019

OPEN ACCESS
CellPress

Cell Reports
Article

LSD1 Interacts with Zfp516 to Promote UCP1 Transcription and Brown Fat Program

Audrey Sambeat,[1] Olga Gulyaeva,[1,2] Jon Dempersmier,[1,3] Kevin M. Tharp,[1] Andreas Stahl,[1] Sarah M. Paul,[1] and Hei Sook Sul[1,2,3,*]
[1]Department of Nutritional Sciences and Toxicology
[2]Endocrinology Program
[3]Comparative Biochemistry Program
University of California, Berkeley, Berkeley, CA 94720, USA
*Correspondence: hsul@berkeley.edu
http://dx.doi.org/10.1016/j.celrep.2016.05.019

SUMMARY

Zfp516, a brown fat (BAT)-enriched and cold-inducible transcription factor, promotes transcription of UCP1 and other BAT-enriched genes for non-shivering thermogenesis. Here, we identify lysine-specific demethylase 1 (LSD1) as a direct binding partner of Zfp516. We show that, through interaction with Zfp516, LSD1 is recruited to UCP1 and other BAT-enriched genes, such as PGC1α, to function as a co-activator by demethylating H3K9. We also show that LSD1 is induced during brown adipogenesis and that LSD1 and its demethylase activity is required for the BAT program. Furthermore, we show that LSD1 ablation in mice using Myf5-Cre alters embryonic BAT development. Moreover, BAT-specific deletion of LSD1 via the use of UCP1-Cre impairs the BAT program and BAT development, making BAT resemble WAT, reducing thermogenic activity and promoting obesity. Finally, we demonstrate an in vivo requirement of the Zfp516-LSD1 interaction for LSD1 function in BAT gene activation.

INTRODUCTION

Unlike white adipose tissue (WAT), whose main function is to store energy in the form of triacylglycerol that is to be used during energy deprivation, brown adipose tissue (BAT) is specialized in heat production for maintenance of body temperature via non-shivering thermogenesis. Since the discovery that active brown-adipose-like tissue is present in adults (Cypess et al., 2009; Farmer, 2009; van Marken Lichtenbelt et al., 2009; Virtanen et al., 2009) and that BAT can have anti-obesity and anti-diabetic effects (Lowell et al., 1993; Enerbäck et al., 1997; Bartelt et al., 2011), mechanisms underlying BAT formation and function have attracted a growing interest in obesity research.

BAT displays high mitochondrial density and contains uncoupling protein 1 (UCP1). UCP1, a proton transporter, uncouples the mitochondrial proton gradient from ATP synthesis, dissipating energy as heat for non-shivering thermogenesis. UCP1 is uniquely expressed in BAT and is induced upon cold exposure. UCP1 transcription is regulated by various transcription factors, such as PPARγ, PGC1α, and ATF2, which can bind to an upstream enhancer region of the UCP1 promoter (Collins et al., 2010; Kang et al., 2005). We recently identified a cold-inducible transcription factor, Zfp516, which is enriched in BAT and activates UCP1 and other BAT-enriched genes, such as PGC1α, to promote a BAT program (Dempersmier et al., 2015). We have shown that Zfp516 activates UCP1 promoter by binding to the proximal region and promotes brown adipogenesis. Consequently, ablation of Zfp516 in mice, although embryonically lethal, showed a drastically reduced BAT depot formation, whereas overexpression of Zfp516 in adipose tissue caused browning of inguinal WAT (iWAT) with increased energy expenditure, preventing diet-induced obesity.

In addition to transcription factors and coregulators, histone modifications (including methylation, phosphorylation, and acetylation) affect chromatin architecture for epigenetic regulation of transcription. LSD1 (also called KDM1A or AOF2) was the first identified histone demethylase, establishing histone methylation as a reversible and dynamic regulatory mechanism for transcription (Wang et al., 2007). LSD1 catalyzes demethylation through a flavin adenosine dinucleotide (FAD)-dependent oxidative reaction and was initially characterized to target mono- and di-methylated K4 residues of histone H3 (H3K4-1me and -2me) (Shi et al., 2004) for transcriptional repression. However, LSD1 has also been shown to promote gene activation through H3K9 demethylation (Metzger et al., 2005). Moreover, LSD1 has been reported to play a role during early stages of white adipocyte differentiation by demethylating H3K9-2me at the C/EBPα promoter region (Musri et al., 2010). Recently, it has been reported that LSD1 is not only essential for early steps of white adipocyte differentiation but promotes oxidative metabolism by interacting with Nrf1 for mitochondrial biogenesis (Duteil et al., 2014). However, the LSD1 function in BAT and whether it can affect UCP1 or BAT gene program remain unclear.

Here, we identify LSD1 as a binding partner of Zfp516. LSD1, which is induced during brown adipogenesis, is recruited to the UCP1 promoter via direct interaction with Zfp516 for transcriptional activation by H3K9 demethylation at the UCP1 promoter region. We also show that LSD1 is required for a BAT gene program, and thus, BAT-specific ablation of LSD1 impairs BAT

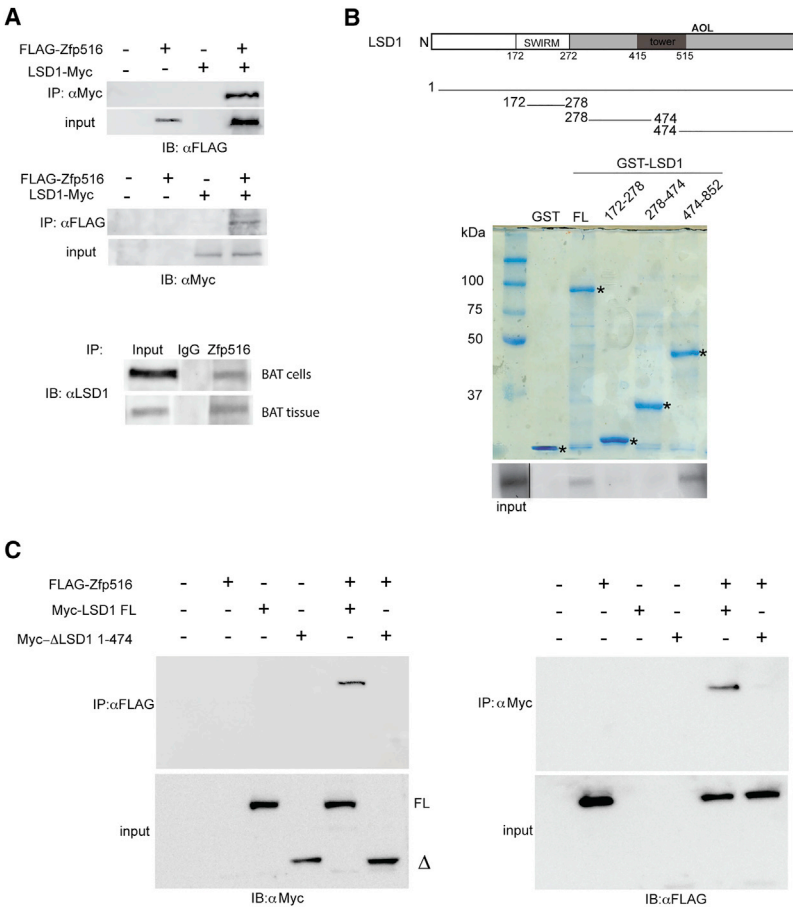

Figure 1. LSD1 Directly Interacts with Zfp516

(A) Immunoblot using αFLAG (Top) or αMyc (Center) after immunoprecipitation with either αMyc or αFLAG, respectively, of HEK293FT cell lysates transfected with FLAG-Zfp516 and c-Myc-LSD1 either together or individually. (Bottom) Immunoblot for endogenous LSD1 after immunoprecipitation of lysates from differentiated BAT cells or BAT tissue with α-Zfp516 is shown.

(B) (Top) Schematic representation of GST-LSD1 deletion constructs. (Center) Coomassie staining for indicated GST constructs is shown. (Bottom) Autoradiograph of GST pull-down using GST fusion proteins containing the indicated domains of LSD1 and ^{35}S-labeled in-vitro-translated Zfp516 is shown. Solid line shows lane position moved within the same blot.

(C) Immunoblot using αMyc (top-left) or αFLAG (top-right) after immunoprecipitation with either αFLAG or αMyc, respectively, of lysates from 293FT cells transfected with FLAG-Zfp516 and either Myc-LSD1 full-length (FL) or deleted Myc-ΔLSD1 1–474 (Δ), together or individually. Immunoblots of input for the corresponding lysate are shown on bottom-left and -right.

See also Figure S1.

program and development in mice. Moreover, we also demonstrate that Zfp516 interacts with LSD1 to promote browning of iWAT in vivo.

RESULTS

We previously reported Zfp516 as a cold-inducible BAT-enriched transcription factor that promotes a BAT gene program. As a DNA-binding protein, Zfp516 may interact with coregulators to activate BAT transcription. Thus, we investigated potential interacting partners of Zfp516 to better understand molecular mechanisms underlying the transcriptional activation of UCP1 and other BAT-enriched genes for promotion of a BAT program.

Direct Interaction between LSD1 and Zfp516

In order to identify Zfp516 binding partners, we used a streptavidin- and calmodulin-binding epitope-tag strategy for tandem affinity purification (TAP) followed by mass spectrometry (MS) analysis. The Zfp516-interacting proteins were purified from lysates prepared from 293FT cells overexpressing Zfp516 tagged with streptavidin- and calmodulin-binding peptides. Lysates from cells overexpressing either TAP alone (empty vector) or TAP-tagged-Zfp516 (TAP-Zfp516) were processed for affinity purification. Eluted proteins were then separated by SDS-PAGE and stained with Coomassie blue (Figure S1A). Bands detected only in TAP-Zfp516 lane were excised and subjected to MS. LSD1 was identified as a candidate-interacting partner of Zfp516.

In order to validate the interaction between LSD1 and Zfp516, we first performed a coimmunoprecipitation (coIP) using 293FT cells transfected with FLAG-tagged-Zfp516 and Myc-tagged-LSD1 either alone or in combination (Figure 1A, top). Indeed, by using FLAG and Myc antibodies, we detected an interaction between Zfp516 and LSD1 only when coexpressed together. We then confirmed interaction between endogenous Zfp516 and LSD1, using lysates from differentiated brown adipocytes as well as BAT from mice. Immunoprecipitation with Zfp516 or LSD1 antibody followed by immunoblotting with LSD1 or Zfp516 antibody, respectively, clearly detected interaction between the two proteins (Figures 1A, bottom, and S1B). Next, we asked whether LSD1 binds Zfp516 directly, by using glutathione S-transferase (GST) fused to LSD1 that was expressed and purified from *E. coli* (Figure 1B, top). By incubating GST-LSD1 fusion protein immobilized on Glutathione Sepharose beads with in-vitro-translated Zfp516, we indeed detected direct interaction between Zfp516 and full-length LSD1 (FL) (Figure 1B, bottom). Furthermore, the use of various GST-LSD1 fragments in the GST assays indicated that LSD1 directly interacts with Zfp516 through a domain located within the C-terminal region of LSD1, aa474–852, containing a part of the tower and amine-oxidase-like (AOL)-C-terminal enzymatic domain (Figure 1B, bottom). Furthermore, when coexpressed with FLAG-Zfp516, the construct lacking aa474–852 (ΔLSD1 1–474) did not coimmunoprecipitate with Zfp516 (Figure 1C, right). Conversely,

immunoprecipitation by FLAG antibody detected LSD1 FL, but not ΔLSD1 1–474 (Figure 1C, left). We conclude that deletion of aa474–852 of LSD1 prevents the interaction of LSD1 with Zfp516. Altogether, these experiments demonstrate the interaction of Zfp516 with LSD1 through the C-terminal domain of LSD1. In this regard, we previously have reported that Zfp516 directly interacts with PRDM16 (Dempersmier et al., 2015). Here, by coIP, we also could detect LSD1 interaction with PRDM16 (Figures S1B and S1C). Overall, these results suggest that, by interacting with Zfp516, PRDM16 and LSD1 are both recruited to the promoter region of UCP1 or other BAT-enriched genes.

By Binding to Zfp516, LSD1 Is Recruited to and Activates the UCP1 Promoter

We previously reported that Zfp516 is recruited to the promoter regions of UCP1 and other BAT-enriched genes, such as PGC1α, for promoter activation. In testing the effect of LSD1 on UCP1 and other BAT genes, we performed luciferase reporter assay using −5.5 kb UCP1 promoter (Figure 2A, top) and −2.4 kb PGC1α promoter (Figure 2A, bottom). Along with the luciferase promoter constructs, Zfp516 and LSD1 were cotransfected, either alone or in combination, into 293FT cells and luciferase activity was measured for quantification. As we previously reported, we observed that Zfp516 activated UCP1 and PGC1α promoter (Figure 2A, top and bottom). In addition, LSD1 alone could also activate these promoters (Figure 2A, top and bottom). More importantly, cotransfection of the promoter constructs with both Zfp516 and LSD1 further increased promoter activity. These results show that Zfp516 and LSD1 work together to activate BAT gene promoters. We next employed two shorter constructs of the UCP1 promoter, which contains Zfp516 binding sequence but lacking the enhancer region of the UCP1 promoter (−70 bp construct), as well as the UCP1 promoter that does not contain neither Zfp516 binding sequence nor the UCP1 enhancer (−45 bp construct; Figure 2B). We found that promoter activation by Zfp516 and LSD1 was detected when cotransfected with the −70-bp construct, but not with the −45-bp construct. These results are consistent with the notion of Zfp516-LSD1 interaction mediating LSD1 activation of UCP1 promoter. We next asked whether LSD1-mediated promoter activation requires enzymatic activity of LSD1 by using a pharmacologic inhibitor of LSD1, 2PCPA, in the reporter assay (Figure 2C). We observed that activation of UCP1 promoter by LSD1 alone or in combination with Zfp516, but not by Zfp516 alone, was greatly reduced in the presence of 2PCPA, indicating the requirement of LSD1 demethylase activity for LSD1 effect on UCP1 promoter activity. In addition, we examined the requirement of Zfp516-LSD1 interaction for promoter activation by cotransfecting 293FT cells with Zfp516 and LSD1 FL or LSD1 deleted of Zfp516 interacting domain, ΔLSD1 1–474 (Figure 2D). We observed a significant decrease in promoter activation for both UCP1 (Figure 2D) and PGC1α (Figure S2B) promoter when Zfp516 binding domain was deleted. Because ΔLSD1 1–474 exhibits similar demethylase activity than LSD1 FL (Figure S2C), this experiment demonstrates the requirement for Zfp516-LSD1 interaction for promoter activation.

Because LSD1 interacts with Zfp516 and induces UCP1 promoter activity, we predicted that LSD1 should occupy the same region that Zfp516 binds within the UCP1 promoter. We performed chromatin immunoprecipitation (ChIP) using BAT cells infected with Zfp516 and LSD1 adenoviruses (Figure 2E). Using FLAG (for Zfp516) and LSD1 antibodies, we detected an enrichment of the −70-bp region of the UCP1 promoter region in comparison to the −5.5-kb region that was used as a control (Figure 2E, left). Quantification by qPCR (primers listed in Table S1) confirmed a 5- and 4-fold enrichment for Zfp516 and LSD1 binding, respectively, to the −70-bp UCP1 promoter region (Figure 2E, center). We next performed reChIP experiment using Zfp516 and LSD1 antibodies sequentially as indicated (Figure 2E, right). We observed enrichment for the −70-bp region of the UCP1 promoter when we first used Zfp516 antibody followed by LSD1 antibody, as well as when we first used LSD1 antibody followed by Zfp516 antibody, whereas no enrichment was observed in the control, GAPDH promoter.

Finally, we tested the requirement of Zfp516 for the LSD1 recruitment to the −70-bp UCP1 promoter region (Figure 2F, left). We compared LSD1 recruitment to the UCP1 promoter region by ChIP using BAT cells in which LSD1 was overexpressed but Zfp516 was knocked down by small hairpin RNA (shRNA) (Figure S2D). We observed a significant decrease in LSD1 binding to the −70-bp region in Zfp516 knockdown cells compared to control cells (Figure 2F, left), whereas there was no binding at the control −5.5-kb region (Figure 2F, right), indicating that Zfp516 is required for LSD1 recruitment to the UCP1 promoter in brown adipocytes.

Transcriptional activation by LSD1 has been shown to be dependent on the demethylation of mono- and di-methylated H3K9 residue (Metzger et al., 2005). Hence, by ChIP, we assessed methylation status of different lysine residues at the UCP1 promoter region (Figure 2G). We compared samples from BAT of mice with BAT-specific LDS1 deletion and their control (fl/fl; described below). We detected higher mono- and di-methylation of H3K9 at the −70-bp region of the UCP1 promoter in BAT from LSD1 knockout (KO) mice (Figure 2G, left). In contrast, H3K9-3me and H3K4-2me at the −70-bp UCP1 promoter region were affected to a lesser extent or not significantly affected (Figure 2G, left). Besides, levels of mono- and di-methylation of H3K9 at the −70-bp region were 8- to 10-fold higher compared to the −5.5-kb promoter region (Figure 2G, right). These observations indicate that LSD1 KO affects lysine methylation specifically at the −70-bp region, consistent with specific LSD1 binding to this region of UCP1 promoter (Figure 2E). Overall, these results support the notion that LSD1 participates in transcriptional activation by modifying histone methylation at the promoter region of BAT-specific UCP1 gene.

Altogether, we conclude that LSD1 is recruited by and cooperates with Zfp516 for the activation of UCP1 promoter. Notably, this activation by LSD1 correlates with demethylation of mono- and di-methylated H3K9 at the promoter region.

LSD1 Is Required for the BAT Gene Program and BAT Development In Vivo

We previously reported that Zfp516 activates UCP1 and other BAT-enriched genes. Thus, Zfp516 ablation causes a decrease in BAT mass with a greatly lower expression of UCP1 and other BAT-enriched genes. If Zfp516 recruits LSD1 for its function,

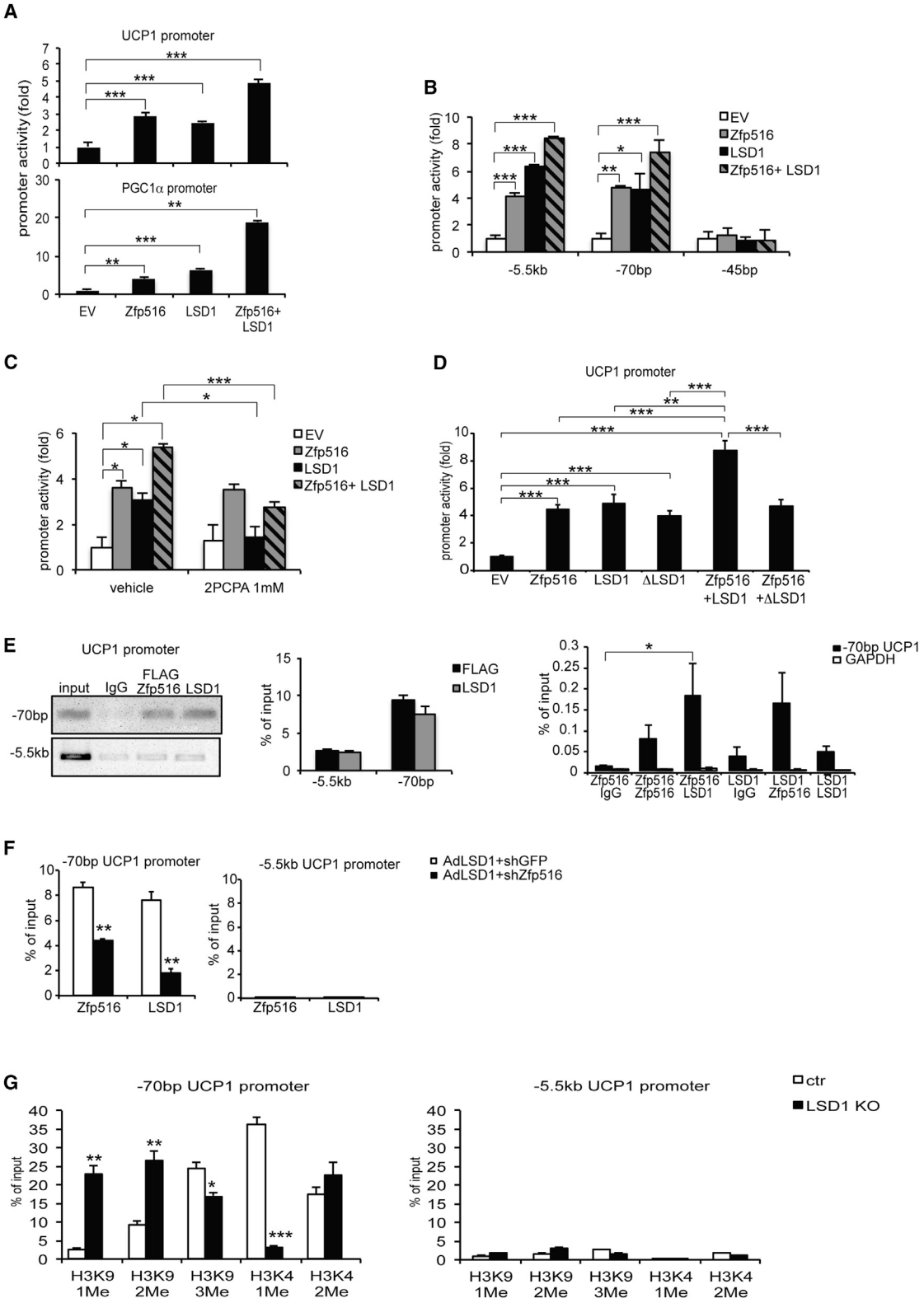

(legend on next page)

LSD1 should also affect expression of BAT-enriched genes. We first compared LSD1 mRNA levels between the stromal vascular fraction (SVF) containing preadipocytes with adipocyte fraction from BAT of 10-week-old wild-type (WT) mice (Figure 3A). As predicted, Pref-1 was found to be higher by 75% in the SVF, whereas UCP1, perilipin, and Zfp516 were 5-, 5-, and 3-fold enriched in adipocyte fraction, respectively. We found LSD1 to be enriched by 4-fold in adipocyte fraction compared to the SVF, implicating an induction of LSD1 during brown adipogenesis. We therefore examined LSD1 mRNA and protein levels during brown adipocyte differentiation of BAT cells in vitro (Figure 3C). As expected, during brown adipocyte differentiation, we observed an increased expression of BAT-enriched genes, such as PGC1α, PRDM16, and Cox8b (Figure 3C, top), as well as common adipocyte differentiation markers, such as PPARγ, FABP4, and adiponectin (AdipoQ; Figure 3C, top). More importantly, LSD1 mRNA level was significantly increased by 5-fold and LSD1 protein level was increased as well, during differentiation (Figure 3C, bottom). We conclude that LSD1 is induced during brown adipocyte differentiation and, thus, LSD1 is enriched in mature brown adipocytes. We also compared expression of LSD1 and Zfp516 in BAT from WT mice after a 6-hr cold exposure at 4°C (Figure 3B). As expected, Zfp516, as well as UCP1 and PGC1α, mRNA levels in BAT were higher by 2.5- to 10-fold upon cold exposure, whereas PRDM16 did not change. Similar to Zfp516, LSD1 mRNA level in BAT was higher by 3-fold upon cold exposure (Figure 3B). Overall, LSD1 expression pattern is similar to Zfp516 in terms of enrichment in mature brown adipocytes and induction by cold, which further supports a cooperative role of LSD1 and Zfp516 for the BAT program.

We next examined the role of LSD1 and its activity during brown adipocyte differentiation in vitro. We treated the cells with two different inhibitors of LSD1, 2PCPA and LSD1i, during brown adipocyte differentiation (Figure 4A). Compared to control vehicle-treated cells, cells treated with LSD1 inhibitors showed lower lipid accumulation (Figure 4A, left-top). Moreover, LSD1 inhibition caused a significant reduction of UCP1 at mRNA (Figure 4A, right) and protein (Figure 4A, left-bottom) levels, as well as decreased expression of other BAT-enriched genes, such as PGC1α, Dio2, PRDM16, Cox8b, and Cidea, by 50%–80% (Figure 4A, right), whereas PPARγ was not affected. These results show that LSD1 demethylase activity is required for expression of BAT-enriched genes and thus BAT gene program.

To further establish the requirement of LSD1 for the BAT gene program and to rule out any off-target effects of LSD1 inhibitors, we next performed adenoviral shRNA-mediated knockdown of LSD1 (Figure 4B). LSD1 was reduced at mRNA (by 70%) as well as at protein level in LSD1-shRNA-infected cells (Figure 4B, left). After 6 days of differentiation, we detected a significantly lower lipid accumulation in shLSD1 cells compared to the control, sh-scrambled cells (Figure 4B, center). Expression level of BAT-enriched genes, such as UCP1, PGC1α, PRDM16, and Cox8b, was lower by 60%–70% (Figure 4B, right-top), whereas common adipose markers, PPARγ and FABP4, were not affected significantly (Figure 4B, right-bottom). The results were confirmed at the protein level. UCP1 and PGC1α levels were drastically reduced, whereas PPARγ level did not change (Figure 4B, left). Taken together, these results demonstrate that LSD1 expression and its enzymatic activity are required for a BAT gene program.

It has been previously reported that global LSD1 KO is lethal by embryonic day 7.5, which prevents further examination of BAT development or function (Wang et al., 2007). Therefore, to evaluate the role of LSD1 in BAT in vivo, we performed a tissue-specific conditional KO of LSD1 using the Cre-*lox* strategy. We first attempted to generate conditional LSD1 KO mice by crossing LSD1-floxed mice with those bearing the Cre recombinase driven by the Myf5 promoter (Tallquist et al., 2000), an established marker of brown adipose precursors (Seale et al., 2008). However, we found that LSD1-Myf5KO resulted in perinatal lethality preventing the study of BAT function in adults. Regardless, we could clearly detect a drastic decrease in the size of BAT depot in Myf5KO newborns compared to control littermates (fl/fl; Figure 4C, left), although the global size of the newborns remained the same (data not shown). LSD1 mRNA level was decreased by 63% in BAT of Myf5KO mice (Figure 4C, left). We also detected a significant decrease in mRNA levels of BAT-enriched genes, such as UCP1, PGC1α, C/EBPβ, and Cox8b, by 25%–60% in BAT of Myf5KO newborns, whereas common adipose markers, such as PPARγ and AdipoQ, were not significantly affected (Figure 4C, right). Thus, we conclude

Figure 2. Zfp516 Recruits LSD1 to Activate the UCP1 Promoter

(A) (Top) Luciferase activity in 293FT cells cotransfected with the −5.5-kb UCP1 promoter or empty vector (EV), along with Zfp516 and LSD1 expression vectors either together or individually. (Bottom) Luciferase activity in cells cotransfected with the −2.4-kb PGC1α promoter or EV along with Zfp516 and LSD1 vectors either together or individually is shown.

(B) Luciferase activity in cells cotransfected with the −5.5-kb, −70-bp, or −45-bp UCP1 promoter or EV, along with Zfp516 and LSD1 vectors either together or individually.

(C) Luciferase activity in cells cotransfected with the −5.5-kb UCP1 promoter and EV, along with Zfp516 and LSD1 vectors either together or individually after treatment with LSD1 inhibitor (2PCPA 1 mM) or vehicle for 48 hr.

(D) Luciferase activity in cells cotransfected with the −5.5-kb UCP1 promoter and EV, along with Zfp516 and either LSD1 FL or deleted ΔLSD1 1–474.

(E) (Left) ChIP for Zfp516 and LSD1 binding at the −70-bp region of UCP1 promoter using both αFlag and αLSD1 for chromatin of BAT cells infected with Zfp516 and LSD1 adenoviruses. The −5.5-kb region of UCP1 promoter was used as a negative control. (Center) qPCR of ChIP DNA is shown. (Right) ReChIP for Zfp516 and LSD1 binding to the UCP1 promoter region in BAT cells using immunoglobulin G (IgG), αZfp516, or αLSD1 as indicated are shown.

(F) (Left) ChIP for Zfp516 and LSD1 binding to the −70-bp region of the UCP1 promoter in BAT cells using both αZfp516 and αLSD1 with LSD1 overexpression and Zfp516 knockdown (shZfp516), compared to negative control (shGFP). (Right) GAPDH promoter was used as a negative control.

(G) ChIP analysis of histone H3 methylations at the −70-bp region of UCP1 promoter (Left) or at the GAPDH promoter as a negative control (Right) in ChIP of BAT tissue from control (fl/fl) or LSD1 KO (LSD1KO) mice.

Data are represented as mean ± SEM. *$p < 0.05$; **$p < 0.01$; ***$p < 0.001$. See also Figure S2.

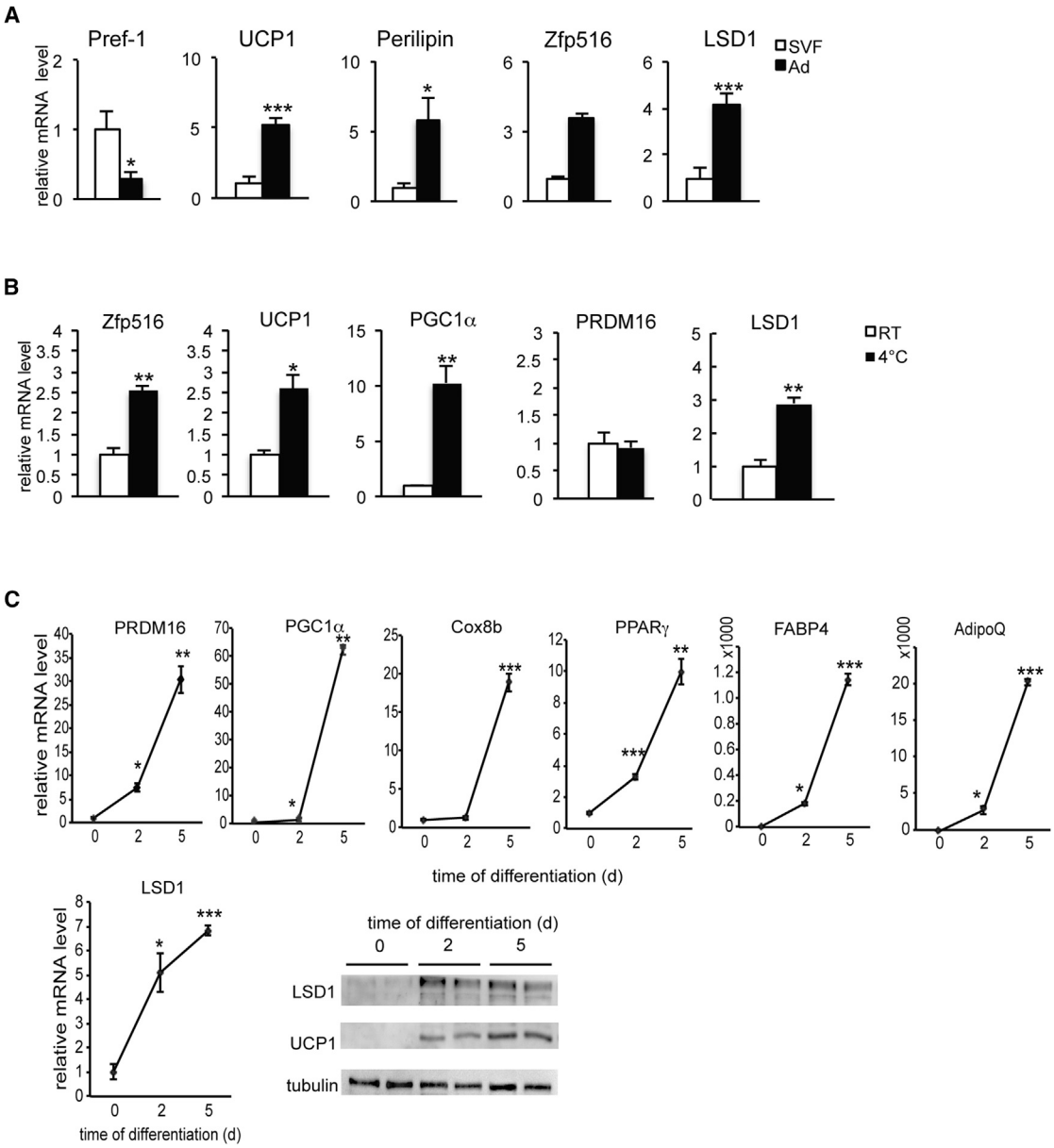

Figure 3. LSD1 Is Increased during Brown Adipocyte Differentiation and Induced by Cold Exposure in BAT

(A) qRT-PCR for indicated gene in the adipocyte fraction and SVF from BAT.

(B) qRT-PCR for indicated gene in BAT of WT mice exposed to cold (4°C) for 6 hr.

(C) (Top) qRT-PCR for indicated gene in BAT cells at days 0, 2, and 5 after the start of differentiation. (Bottom) LSD1 mRNA level (Top) and immunoblot (Bottom) for indicated proteins in BAT cells at days 0, 2, and 5 of differentiation are shown.

Data are represented as mean ± SEM. *p < 0.05; **p < 0.01; ***p < 0.001.

that LSD1 ablation in brown adipose precursors impairs embryonic development of BAT in vivo.

LSD1 Promotes a BAT Gene Program and Thermogenesis In Vivo

To further evaluate the role of LSD1 in BAT development and its function in vivo, we performed conditional KO of LSD1 using different Cre mice to overcome perinatal lethality of our Myf5KO model (Figure 4C). Because UCP1 has been shown to express early during BAT development, we next employed UCP1-Cre. Crossing LSD1-floxed mice with mice carrying the UCP1 promoter-Cre (Kong et al., 2014) produced BAT-specific KO mice (BSKO) at room temperature, allowing us to examine the role of LSD1 in BAT. In addition to genotyping, we further validated our mouse model by measuring LSD1 mRNA levels in BAT of LSD1-BSKO and $LSD1^{fl/fl}$ control (fl/fl) mice. LSD1 mRNA level was decreased by 65% in BAT, but not in WAT depots, iWAT and perigonadal WAT (pWAT) (Figure 5B, top-left). Similarly,

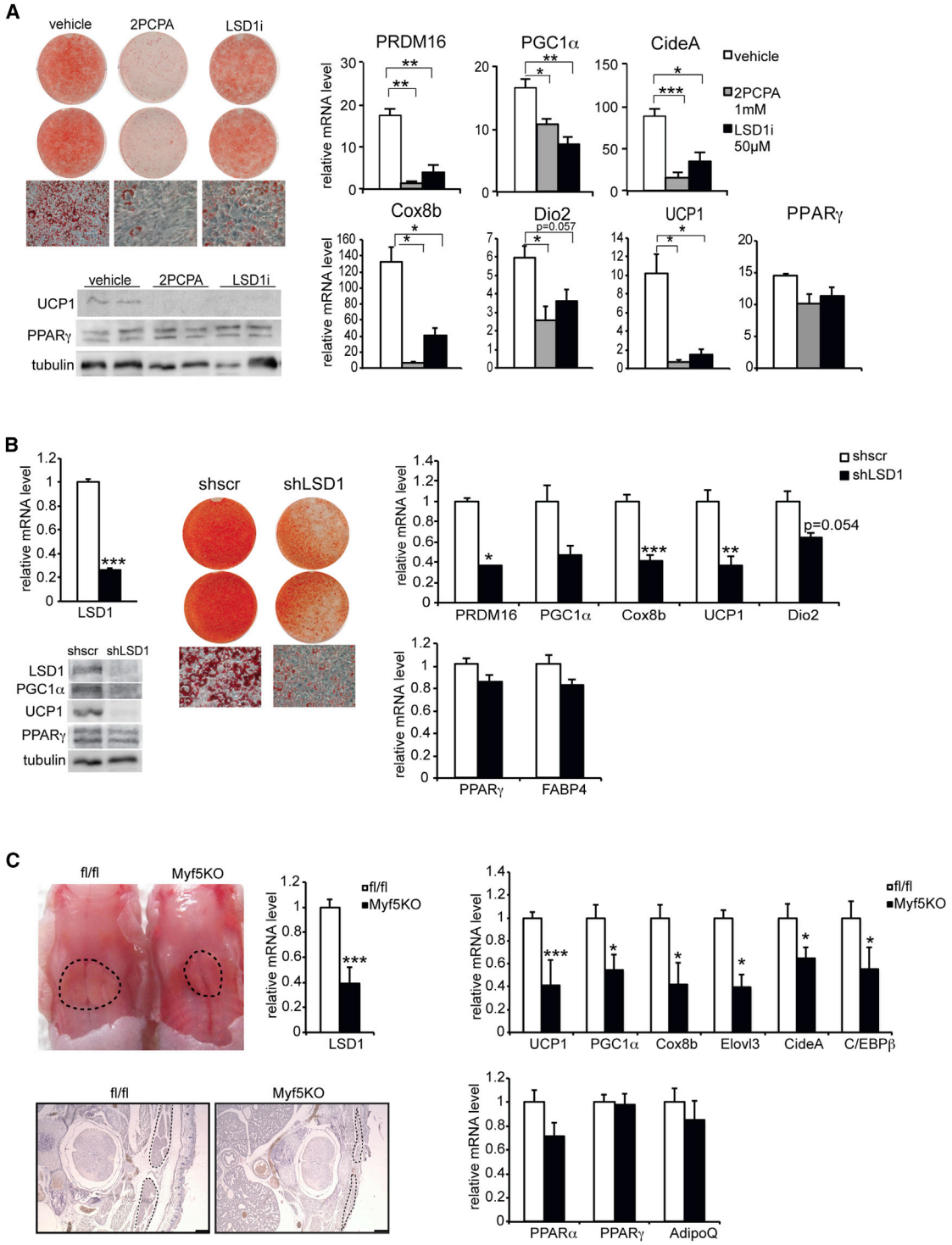

Figure 4. LSD1 Is Required for the BAT Program and BAT Development

(A) (Left-top) ORO staining and bright-field view (20× magnification) of BAT cells treated with vehicle (left panel) or LSD1 inhibitors: 2PCPA (Center) and LSD1i (Right), at day 6 of differentiation. (Left-bottom) Immunoblotting for indicated proteins in lysates from BAT cells at day 6 is shown. (Right) qRT-PCR for indicated genes in BAT cells treated with vehicle (Left) or LSD1 inhibitors at day 6 is shown.

(B) (Left) qRT-PCR for LSD1 mRNA in BAT cells infected with control scrambled (shscr) or shLSD1 adenovirus at day 6 (Top). Immunoblot for indicated proteins in BAT cells at day 6 (Bottom) is shown. (Center) ORO staining and bright-field views (20× magnification) of BAT cells infected with control shscr (Left) or shLSD1 (Right) adenovirus at day 6 are shown. (Right) qRT-PCR for indicated genes in BAT cells infected with control shscr or shLSD1 adenovirus at day 6 is shown.

(legend continued on next page)

LSD1 protein level was reduced only in BAT, but not in liver, iWAT, or pWAT (Figure 5B, top-right), showing the BAT specificity of the model.

LSD1-BSKO mice exhibited a significantly higher body weight by approximately 4 g than control littermates (Figure 5A, top) at 14 weeks, whereas food intake was not affected (Figure S3A). Their BAT depot was bigger but pale (right) in comparison to control mice (left; Figure 5A, top). Body composition analysis indicated that, whereas fat mass was increased, lean mass remained the same in BSKO mice (Figure 5A, center and bottom). Histological analysis of the BAT depot from BSKO mice had noticeable morphological differences. H&E staining showed BAT of BSKO mice exhibited bigger lipid droplets in comparison to control littermates (Figure 5C, center). Interestingly, whereas BAT from control mice presented brown adipocytes with small lipid droplets, which is typical of BAT, BAT from BSKO mice exhibited adipocytes containing bigger lipid droplets. Morphology of WAT, as demonstrated with H&E staining of pWAT sections, was unchanged (Figure 5C, top). Furthermore, expression levels of BAT-enriched genes, such as PGC1α, UCP1, CideA, and Cox8b, were lower by 55%–30% (Figure 5B, center), whereas common adipocyte markers, PPARγ, FABP4, AdipoQ, and perilipin, were not affected (Figure 5B, bottom). Immunoblots showed a strong reduction of UCP1 at the protein level only in BAT and not in WAT, whereas PPARγ remained unchanged (Figure 5B, top-right). Similarly, immunostaining for UCP1 showed a correspondingly lower staining in BSKO compared to control mice (Figure 5C, bottom). Collectively, BAT of LSD1-BSKO mice lost the major BAT phenotypic characteristics of brown coloration, presence of multiple lipid droplets within smaller adipocytes, and BAT gene expression pattern. Moreover, not only did we observe a loss of BAT characteristics, but we also observed a switch toward a more-white-adipose-specific morphology of bigger lipid droplet size with increased lipid content. Overall, these results demonstrate that LSD1 ablation causes a whitening of BAT, establishing in vivo requirement of LSD1 for a normal BAT program.

Considering that LSD1-BSKO mice had no change in food intake but exhibited a higher body weight, we next investigated whether energy expenditure could be altered. We first evaluated thermogenic capacity by measuring body temperature. We found that LSD1-BSKO mice had a lower body temperature than control mice at room temperature, and this difference in body temperature was further enhanced after a 6-hr cold exposure (Figure 5D). These results suggest an impaired thermogenic function of BSKO mice. Indeed, indirect calorimetry showed that oxygen consumption (VO_2) was significantly reduced in BSKO mice compared to WT mice at room temperature, whereas respiratory ratio and locomotor activity were unchanged (Figures 5E, left, S3B, and S3C). Similar reduction in oxygen consumption was observed at thermoneutrality (30°C), as well as at 4°C (Figure S3D). Taken together, we conclude that energy expenditure estimated by oxygen consumption was decreased in LSD1-BSKO mice compared to control mice. To examine the contribution of BAT to the altered energy expenditure in BSKO mice, we next measured oxygen consumption rate (OCR) of BAT dissected out from these LSD1-BSKO mice (Figure 5E, right). Indeed, we found significantly lower OCR in BAT from BSKO mice by 35% in comparison to that from control mice. In line with these results, BSKO mice gained more body weight on high-fat diet (HFD) than their control littermates, demonstrating a propensity for obesity upon BAT-specific LSD1 deletion (Figure 5F, left). In addition, blood glucose level of BSKO mice on HFD measured in the course of a glucose tolerance test (GTT) was significantly higher than in control littermates (Figure 5F, right), indicative of an impaired glucose tolerance. Collectively, these data establish a defective BAT function in BSKO mice and that LSD1 ablation reduced thermogenic capacity in vivo. Furthermore, in evaluating the role of LSD1 in BAT, we also generated LSD1 conditional KO mice by mating the LSD1-floxed mice with AdipoQ-Cre mice (Eguchi et al., 2011) for LSD1 KO in all adipose tissue depots BAT, iWAT and pWAT (ASKO mice; Figure S4). We found the phenotype of these ASKO mice to be quite similar to that in BSKO mice (Figure S4), thus further confirming the critical role of LSD1 for BAT function.

In Vivo Requirement of LSD1-Zfp516 Interaction

To demonstrate the significance of LSD1-Zfp516 interaction, we tested LSD1 requirement in the context of Zfp516-induced browning of iWAT. In this regard, we previously have shown that overexpression of Zfp516 in adipose tissue causes browning of iWAT. In testing the requirement of LSD1 on Zfp516-induced browning, we performed a LSD1 knockdown in 3T3-L1 cells overexpressing Zfp516 (AdZfp516) or a control empty GFP vector (AdGFP) (Figure 6A). We verified Zfp516 overexpression and LSD1 knockdown at both mRNA (35- to 40-fold and 70%, respectively) and protein levels (Figure 6A, top). We observed that induction of BAT-enriched genes by Zfp516 overexpression was impaired in LSD1 shRNA knockdown cells (shLSD1) compared to control shRNA (shscr) cells, as indicated by approximately 50% decrease in mRNA levels for PGC1α, UCP1, and Cidea (Figure 6A, bottom), as well as strong reduction of UCP1 at protein level (Figure 6A, top-right). Next, to evaluate the requirement of LSD1 within in vivo setting, we performed implantation experiments using Zfp516-overexpressing 3T3-L1 cells coinfected with shLSD1 or control shscr (Figure 6B). After 7 days, implants along with pWAT as a control were collected and analyzed. Zfp516 overexpression and LSD1 knockdown were validated at the mRNA levels, as indicated by 8- to 10-fold increase in Zfp516 mRNA level and 55% decrease in LSD1 in knockdown implants (Figure 6B, left-top). The expression of BAT-enriched genes, such as PGC1α, UCP1, Elovl3, and Dio2, was greatly reduced in shLSD1 knockdown implants compared to control, at a level close to that in pWAT depot

(C) (Top-left) Representative photograph of control (fl/fl) and LSD1$^{fl/fl}$-Myf5Cre (Myf5KO) newborn embryos (P0) from back view. Black dots delineate area of BAT. qRT-PCR for LSD1 mRNA in BAT of control and Myf5KO embryos (n = 8–9 embryos per group) is shown. (Bottom-left) H&E staining of representative transversal sections of the interscapular region of control and Myf5 KO embryos (P0) is shown. Black dots delineate area of BAT. (Right) qRT-PCR for BAT-enriched (Top) and common adipose genes (Bottom) in BAT of control or Myf5KO embryos (n = 8–9 embryos per group) is shown.
Data are represented as mean ± SEM.*p < 0.05; **p < 0.01; ***p < 0.001.

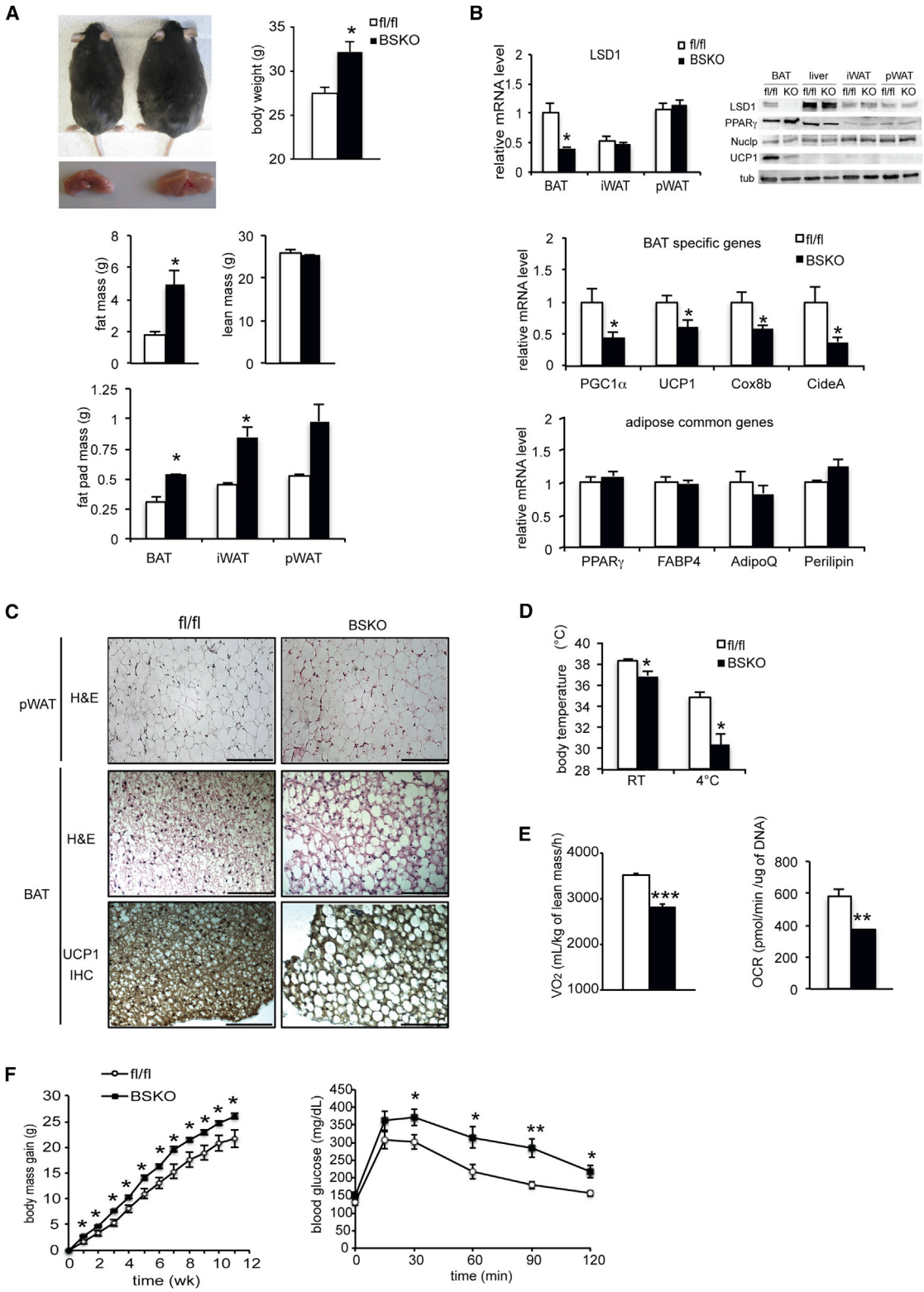

Figure 5. LSD1 Promotes a BAT Gene Program In Vivo

(A) (Top-left) Representative photograph of control and LSD1 BSKO 17-week-old mice and their BAT depot. (Top-right) Body weight of 14-week-old control and LSD1 BSKO mice is shown. (Center) Fat and lean mass of 14-week-old control and LSD1 BSKO mice determined using EchoMRI is shown. (Bottom) Mass of adipose depots from mice described above is shown.

(legend continued on next page)

(Figure 6B, right-top). However, we did not observe any difference in PPARγ expression between these implants (Figure 6B, right-bottom). Moreover, histological analysis of implant sections showed a global increase in adipocyte size, as well as decreased UCP1 staining in shLSD1 implants (Figure 6B, left-bottom). These results suggest that Zfp516 and LSD1 cooperate together to activate BAT-enriched genes in white adipocytes, thereby changing their characteristics toward a brown morphology. Furthermore, upon exposure of LSD1-ASKO mice at 4°C for 6 hr, we observed expression of BAT-enriched genes, such as PGC1α, UCP1, and Cox8b, was lower not only in BAT (Figures S5A and S5C) but also iWAT of ASKO mice in comparison to control littermates (Figures S5A and S5B). These results demonstrate a role for LSD1 in cold-induced browning of iWAT, in addition to promotion of thermogenic program in BAT as shown above. To address the relevance of Zfp516-LSD1 interaction for iWAT browning in a more physiologically relevant system, we generated an additional mouse model by crossing aP2-Zfp516 transgenic mice overexpressing Zfp516 in all adipose depots with LSD1-ASKO mice with LSD1 ablation in all adipose depots (Figure 6C). We verified Zfp516 overexpression and LSD1 ablation in iWAT of aP2-Zfp516, aP2-Zfp516 ASKO, and their control littermates (fl/fl). We detected a 160- to 200-fold increase in Zfp516 expression and 60% lower LSD1 expression, respectively, in these mice (Figure 6C, left-top). Zfp516 overexpression and LSD1 KO in iWAT were confirmed at the protein level (Figure S6B). We found that induction of BAT-enriched genes, including UCP1, Cox8b, and PGC1α, by Zfp516 in iWAT was blunted upon LSD1 ablation, whereas adipose common markers for WAT and BAT, such as PPARγ and AdipoQ, remained unchanged (Figure 6C, right). Histological analysis of iWAT sections showed that LSD1 ablation prevented morphological changes (smaller lipid droplets) and UCP1 staining arising from Zfp516 overexpression in aP2-Zfp516-LSD1-ASKO mice (Figure 6C, left-bottom). In comparison, there was no drastic change in either morphology or UCP1 staining in pWAT (Figure S6A). Moreover, as expected, LSD1 ablation also reduced the expression of BAT-enriched genes in BAT of aP2-Zfp516 mice (Figure S6C). Collectively, these results demonstrate the role of LSD1 in the induction of the BAT program and browning of iWAT in vivo and, more importantly, the biological significance of LSD1-Zfp516 interaction in these processes.

DISCUSSION

In the present study, we demonstrate that Zfp516, previously established as a transcriptional activator of UCP1 and other BAT-enriched genes, directly interacts with LSD1. Zfp516 recruits LSD1 on the promoter regions of BAT genes, and they work together for transcriptional activation of BAT genes. In this context, LSD1 works as a coactivator for the regulation of BAT genes through its demethylase activity on H3K9. We establish both in vitro and in vivo that LSD1 is crucial for the BAT program for proper development and function of BAT. Altogether, our data establish that LSD1 is a cold-induced histone modifier interacting with Zfp516, a BAT-enriched transcription factor, for its recruitment and thereby regulates transcription of BAT genes. We demonstrate here the requirement of LSD1 for Zfp516 function in inducing a BAT program to promote thermogenic function of BAT and also browning of iWAT.

Whereas LSD1 has been initially described as a component of a repressor complex by removing active epigenetic marks by demethylating H3K4 (H3K4-1me and -2me), it has also been reported that LSD1 can act as a coactivator by demethylating H3K9 (H3K9-1me and -2me). We show here that, in the context of BAT gene regulation, LSD1 works as a coactivator recruited by Zfp516, and we detected increased H3K9-1me and H3K9-2me, but not of H3K4-1me and H3K4-2me, at the promoter region of UCP1 in BAT of LSD1 KO mice. We observed no increase but rather a decrease in H3K4-1me in LSD1 BSKO BAT, which may have resulted from altered expression or activity of other methylase(s) due to impaired brown adipogenesis. In this regard, G9a methyltransferase has been reported to induce PPARγ expression during both white and brown adipogenesis by methylating H3K9-1me (Wang et al., 2013). EHMT1, a methyltransferase that has recently been shown to regulate brown adipose cell fate, may also affect histone modification (Ohno et al., 2013). Considering that many methylases and demethylases act together to regulate histone methylation for transcriptional activation, the decrease observed in H3K4-1me is likely an indirect effect of LSD1 KO on other histone methylases at the same region of UCP1 promoter. Notably, it has been reported that LSD1 affects histone methylation status in association with SETDB1 histone methylase on C/EBPα promoter during white adipogenesis (Musri et al., 2010). Regardless, histone demethylases and methyltransferases may target the same residues to maintain a tightly regulated balance between activating and repressive epigenetic marks on BAT gene promoters.

Our results suggest that LSD1 activates UCP1 and other BAT genes, such as PGC1α, probably by demethylating H3K9-1me and H3K9-2me, which are known to be epigenetic repressive marks. It remains unclear how LSD1 mediates transcription repression or activation, either by demethylating H3K4 or H3K9, respectively. Recently, it has been reported that an

(B) (Top) qRT-PCR for LSD1 mRNA in adipose tissue depots of control and LSD1 BSKO mice (Left) and immunoblot for indicated proteins BAT, liver, iWAT, and pWAT of control and LSD1 BSKO mice (Right). (Center) qRT-PCR for BAT-enriched genes in BAT of control and LSD1 BSKO mice is shown. (Bottom) qRT-PCR for common adipose genes in BAT of control and LSD1 BSKO mice is shown.

(C) H&E staining of pWAT sections from control and LSD1 BSKO mice (Top). H&E staining (Center) and immunostaining for UCP1 (Bottom) of BAT sections from control and LSD1 BSKO mice are shown.

(D) (Top) Body temperature from control and LSD1 BSKO mice at 23°C and after a 6-hr cold exposure at 4°C.

(E) (Left) VO_2 consumption measured by indirect calorimetry in control and LSD1 BSKO mice on chow diet (NCD) at room temperature (23°C; n = 7 mice per group). (Right) Oxygen consumption rate (OCR) of BAT from control and LSD1 BSKO mice.

(F) (Left) Body mass gain of control and BSKO mice under HFD starting at 6 weeks of age (n = 6–8 mice per group). (Right) GTT on 16-week-old control and BSKO mice under HFD for 10 weeks is shown (n = 6–8 mice per group).

The scale bars represent 200 μm. Data are represented as mean ± SEM. *$p < 0.05$; **$p < 0.01$; ***$p < 0.001$. See also Figure S3.

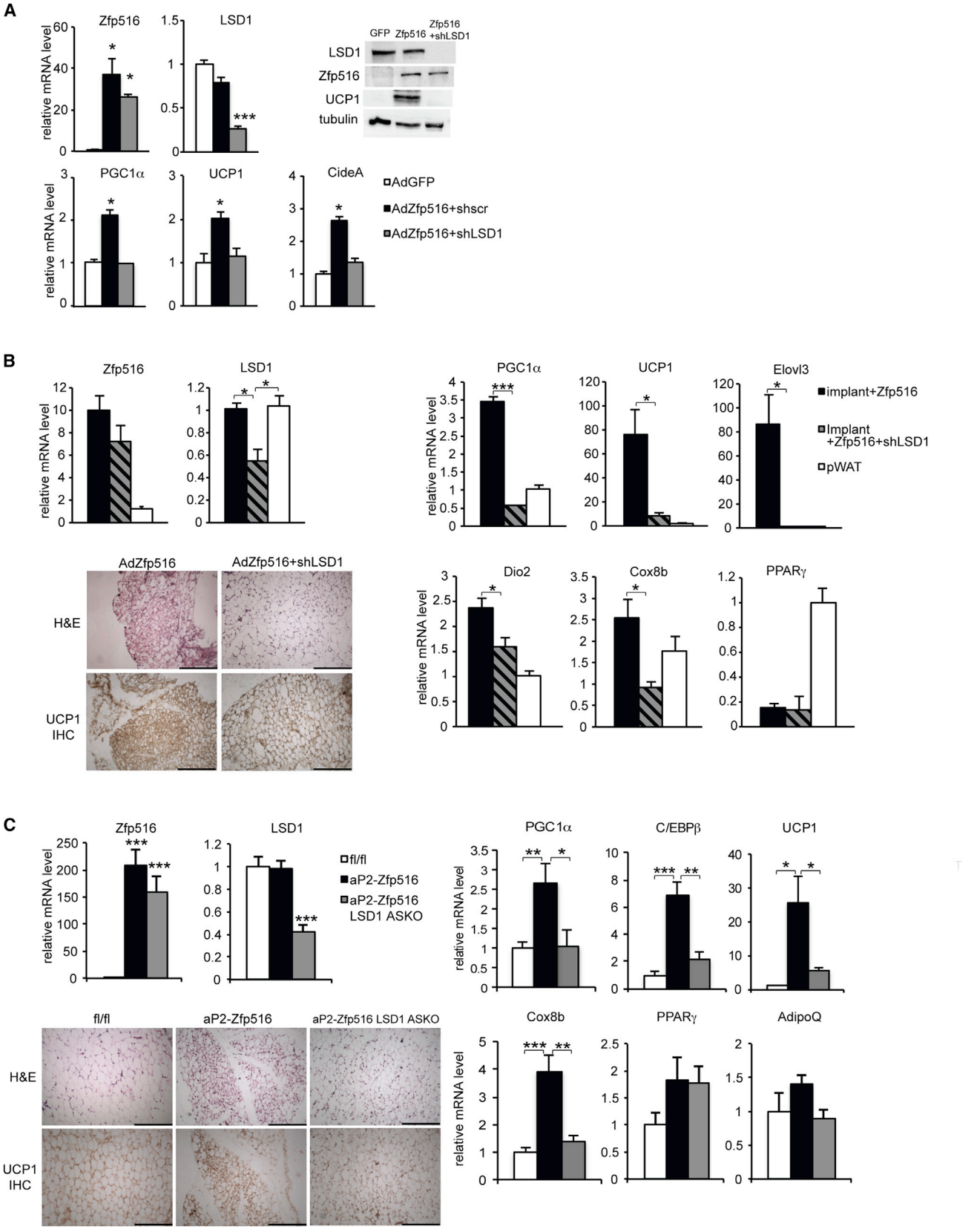

(legend on next page)

isoform of LSD1, LSD1+8a arising from alternative splicing, does not retain any enzymatic activity toward H3K4-2me and hence regulates neuronal differentiation solely through demethylation of H3K9-2me (Laurent et al., 2015). Another study documented LSD1+8a to demethylate H4K20, which was associated with memory and learning process (Wang et al., 2015). Regardless, we could not detect LSD1+8a isoform either in BAT or in differentiated BAT cells (data not shown). Such a versatile substrate specificity of LSD1 remains to be elucidated. We propose that Zfp516 controls LSD1 specificity by recruiting it to chromatin to demethylate H3K9 at the promoter regions for BAT development and function.

We show here that Zfp516 directly interacts with LSD1, thereby recruiting it to the promoter regions of UCP1 or other BAT-enriched genes. Thus, LSD1 activates thermogenic genes, such as UCP1 and PGC1α, for BAT program. Interestingly, Duteil et al. (2014), globally overexpressed LSD1 in mice and reported that LSD1 promotes oxidative capacities in WAT by interaction with nuclear respiratory factor 1 (Nrf1) for mitochondrial biogenesis. In the same study, LSD1 was reported also to induce Nrf1 expression for the observed effect. Due to the global overexpression of LSD1 in these mice, however, specific role of LSD1 in WAT was not clear. In this regard, we previously have shown that Zfp516 overexpression in adipose tissue causes browning of iWAT. We cannot rule out that LSD1 may function by interacting with multiple partners. However, because LSD1 directly interacts with Zfp516 and both of these genes are cold-inducible, iWAT browning may be mediated by LSD1-Zfp516 interaction. Indeed, we found that knockdown of LSD1 in 3T3-L1 cells prevented Zfp516-induced BAT gene activation, indicating involvement of Zfp516-LSD1 interaction in this process (Figure 6A). LSD1 ablation prevents Zfp516-induced browning of implanted 3T3-L1 cells (Figure 6B) but also of iWAT in aP2-Zfp516 LSD1 ASKO mice (Figure 6C). Hence, we show here that LSD1 is required for browning of iWAT through its interaction with Zfp516. Not only LSD1 but Zfp516 also have multiple interacting partners. We previously reported that Zfp516 directly interacts with PRDM16 for transcriptional activation of UCP1 and other BAT-enriched genes, such as PGC1α. Here, we confirmed that LSD1 interacts with PRDM16 (Figure S1B). More importantly, we demonstrate that Zfp516 function requires interaction with LSD1. Therefore, we propose that multiple coregulators, such as LSD1 and PRDM16, interact with Zfp516 in inducing BAT genes for BAT program and thermogenesis.

In order to examine the role of LSD1 during BAT development in vivo, we first attempted at generating LSD1 conditional KO in brown adipose precursors using Myf5-Cre mice. However, LSD1 Myf5KO mice were found to die perinatally. Such an early lethality might have resulted from the fact that, besides brown adipose precursors, Myf5$^+$ cells are early mesenchymal progenitors giving rise to myocytes, cartilage, and dermis. Interestingly, LSD1 has been shown to regulate myogenesis through regulation of MyoD and Mef2 expression (Choi et al., 2010) as well as thyroid hormone signaling (Ambrosio et al., 2013). We propose that survival of LSD1 Myf5KO pups was probably compromised not only by impaired thermoregulation but also by defects in development of other tissues. Unlike previously characterized ASKO mice using aP2 promoter, which were shown to be devoid of WAT (Duteil et al., 2014), our ASKO mice with adiponectin-Cre promoter exhibited an increase in WAT mass. Considering that AdipoQ is expressed later than aP2/FABP4 during development, LSD1 may be crucial only for early steps of WAT development, which is in accordance with previously reported in vitro studies (Duteil et al., 2014). We predict that impaired BAT development and function in these mice may have caused increase in lipid content and depot size of WAT as a compensatory mechanism. Regardless, we cannot rule out other role of LSD1 in WAT, such as that reported by Duteil et al. As is the case of coregulators in general, LSD1 may function with other transcription factors, such as Nrf1, in WAT to alter fatty acid (FA) oxidation and thus lipid content. The use of UCP1-Cre allows ablation of LSD1 in BAT (UCP1$^+$ cells specifically), when mice are maintained at room temperature. Upon cold exposure, LSD1 could be ablated in subcutaneous WAT depots of BSKO mice also, with the appearance of UCP1-expressing beige cells. BAT-conditional KO (BSKO mice) shows a stronger phenotype in BAT and WAT than Myf5-PRDM16KO. Indeed, Harms et al. (2014) reported that Myf5-PRDM16 KO mice exhibit a late-onset decrease of thermogenic markers in BAT, suggesting that PRDM16 is dispensable for early BAT development but required for BAT identity maintenance. However, they suggested compensatory activity of PRDM3 in PRDM16 KO mice and reported a stronger phenotype in PRDM16/PRDM3 double KO mice. Similarly, UCP1 KO mice (Enerbäck et al., 1997) phenotype is milder than LSD1 BSKO. However, only UCP1 is deleted and, as the authors indicated, UCP2 was induced for compensation. These points may explain the differences in phenotype severity. However, we also suggest that, because of Zfp516-LSD1 interaction, the phenotype we observed in LSD1 BSKO is also due to the impaired Zfp516 function for activation of UCP1 and BAT-enriched genes and BAT development.

In conclusion, our results support the idea that BAT development and function require the concerted action of transcriptional regulators as well as chromatin modifiers. We establish that, not

Figure 6. Zfp516-LSD1 Interaction Is Required for Browning of iWAT

(A) (Top) qRT-PCR for LSD1 and Zfp516 mRNA in 3T3-L1 cells coinfected with either control AdGFP or AdZfp516 and control shscr or shLSD1 adenovirus at day 7 of differentiation (left). Immunoblot for indicated proteins in lysates from infected 3T3-L1 cells at day 7 (right). (Bottom) qRT-PCR for BAT-enriched genes in infected 3T3-L1 cells at day 7 is shown.

(B) (Left) qRT-PCR for LSD1 and Zfp516 mRNA in implants and pWAT from mice implanted with 3T3-L1 cells infected with either AdZfp516 + shscr (control) or AdZfp516 + shLSD1 (Top). H&E staining (Top) and immunostaining for UCP1 (Bottom) of sections of implants described above (Bottom) are shown. (Right) qRT-PCR for BAT-enriched genes and adipose common genes in implants and pWAT described above (n = 6 mice per group).

(C) (Left) qRT-PCR for LSD1 and Zfp516 mRNA in iWAT from 8-week-old control (fl/fl), aP2-Zfp516, and aP2-Zfp516 ASKO mice (n = 6–8 mice per group). H&E staining (Top) and immunostaining for UCP1 (Bottom) in sections of iWAT from mice described above are shown. The scale bars represent 200 μm. (Right) qRT-PCR for BAT-enriched or common adipose genes in iWAT from mice described above is shown.

Data are represented as mean ± SEM.*$p < 0.05$; **$p < 0.01$; ***$p < 0.001$. See also Figures S4–S6.

only is LSD1 required for BAT development, but it is also a major activator of BAT-enriched genes through its interaction with Zfp516, thereby regulating thermogenesis. As both Zfp516 and LSD1 are cold inducible, it reinforces the idea that their interplay is essential for cold adaptation. Thus, Zfp516 directly interacts with LSD1 and recruits it to BAT gene promoters, where it demethylates H3K9 residues. Together, they promote a BAT gene program and regulate both development and thermogenic function of BAT as well as browning of iWAT.

EXPERIMENTAL PROCEDURES

Animals

Mice carrying floxed LSD1 alleles (KDM1a $^{fl/fl}$), UCP1-Cre, adiponectin-Cre (AQ-Cre), Myf5-Cre transgenic, and Swiss SWR/J mice were obtained from The Jackson Laboratory. aP2-Zfp516 transgenic mice were described previously (Dempersmier et al., 2015). All protocols for mice studies were approved from the University of California at Berkeley Animal Care and Use Committee. Mice were fed a chow diet or an HFD (45% calorie from fat; Research Diet) ad libitum. Body weight and food intake were measured weekly. See also Supplemental Experimental Procedures.

Cell Transplantation

3T3-L1 cells expressing *Luciferin* were implanted in Swiss SWR/J-recipient mice using a matrix-assisted cell transplantation strategy described previously (Tharp et al., 2015). Briefly, 3T3-L1 Luc cells were infected with AdZfp516 and either Adshscr or AdshLSD1 as in Orlicky and Schaack (2001). Forty-eight hours post-infection, cells were resuspended in hydrogel at 3 × 10^6 cells/ml and 100 μl was injected into subcutaneous inguinal region of recipient mice. After 7 days, implants were collected along with pWAT for further mRNA extraction and histological analysis.

Body Composition and Histology

Body composition was measured in non-anesthetized mice using MRI (EchoMRI). For histology, fresh tissues were fixed in 4% paraformaldehyde, embedded in paraffin, sectioned in 5-μM-thick sections, and stained with H&E. For immunohistochemistry, fresh tissues were fixed in 7% glutaraldehyde, included in optimal cutting temperature compound (OCT), and sectioned on Leica CM3050S Cryostat in 20-μm-thick sections further incubated with αUCP1.

Indirect Calorimetry, Explant Respiration, and Body Temperature

Oxygen consumption (VO_2) was measured using the Comprehensive Laboratory Animal Monitoring System (CLAMS) (Colombus Instruments). Data were normalized to lean body mass determined by EchoMRI. Tissue explant respiration was measured using a XF24 Analyzer (Seahorse Bioscience). Briefly, 3- to 5-μg pieces of tissue were placed into KREB's-Heslinger buffer in XF-24 plates with an islet capture screen and incubated for 1 hr at 37°C without CO_2 prior to analysis. Body temperature was assessed using a RET-3 rectal probe for mice (Physitemp).

GTTs

For GTTs, mice were fasted overnight. Glucose (1 mg/g) was administered intraperitoneally. Blood glucose was measured at indicated time.

Statistical Analysis

Data are expressed as means ± SEM. The statistical differences in mean values were assessed by Student's t test. The sample size was six to eight per genotype for animal studies and three to six for protein and transcript. All experiments were performed at least three times, and representative data are shown.

SUPPLEMENTAL INFORMATION

The Supplemental Information includes the Supplemental Experimental Procedures and six figures and can be found with this article online at http://dx.doi.org/10.1016/j.celrep.2016.05.019.

AUTHOR CONTRIBUTIONS

H.S.S. and A. Sambeat designed the project and wrote the manuscript. A. Sambeat performed all experiments. O.G. performed coIP, reporter assays, and subcloning. J.D. performed ReChIP. K.M.T. and A. Stahl performed cell transplantation. S.M.P. performed the TAP assay.

ACKNOWLEDGMENTS

We thank Y. Shi and J. Lingner for GST-LSD1 constructs. We thank S. Kajimura for BAT brown preadipocyte cell line. We thank T. Do and S. Yoo for technical assistance. The work was supported in part by DK095338 to H.S.S.

Received: August 31, 2015
Revised: February 4, 2016
Accepted: May 2, 2016
Published: June 2, 2016

REFERENCES

Ambrosio, R., Damiano, V., Sibilio, A., De Stefano, M.A., Avvedimento, V.E., Salvatore, D., and Dentice, M. (2013). Epigenetic control of type 2 and 3 deiodinases in myogenesis: role of lysine-specific demethylase enzyme and FoxO3. Nucleic Acids Res. *41*, 3551–3562.

Bartelt, A., Bruns, O.T., Reimer, R., Hohenberg, H., Ittrich, H., Peldschus, K., Kaul, M.G., Tromsdorf, U.I., Weller, H., Waurisch, C., et al. (2011). Brown adipose tissue activity controls triglyceride clearance. Nat. Med. *17*, 200–205.

Choi, J., Jang, H., Kim, H., Kim, S.T., Cho, E.J., and Youn, H.D. (2010). Histone demethylase LSD1 is required to induce skeletal muscle differentiation by regulating myogenic factors. Biochem. Biophys. Res. Commun. *401*, 327–332.

Collins, S., Yehuda-Shnaidman, E., and Wang, H. (2010). Positive and negative control of Ucp1 gene transcription and the role of β-adrenergic signaling networks. Int. J. Obes. (Lond) *34*, S28–S33.

Cypess, A.M., Lehman, S., Williams, G., Tal, I., Rodman, D., Goldfine, A.B., Kuo, F.C., Palmer, E.L., Tseng, Y.H., Doria, A., et al. (2009). Identification and importance of brown adipose tissue in adult humans. N. Engl. J. Med. *360*, 1509–1517.

Dempersmier, J., Sambeat, A., Gulyaeva, O., Paul, S.M., Hudak, C.S., Raposo, H.F., Kwan, H.Y., Kang, C., Wong, R.H., and Sul, H.S. (2015). Cold-inducible Zfp516 activates UCP1 transcription to promote browning of white fat and development of brown fat. Mol. Cell *57*, 235–246.

Duteil, D., Metzger, E., Willmann, D., Karagianni, P., Friedrichs, N., Greschik, H., Günther, T., Buettner, R., Talianidis, I., Metzger, D., and Schüle, R. (2014). LSD1 promotes oxidative metabolism of white adipose tissue. Nat. Commun. *5*, 4093.

Eguchi, J., Wang, X., Yu, S., Kershaw, E.E., Chiu, P.C., Dushay, J., Estall, J.L., Klein, U., Maratos-Flier, E., and Rosen, E.D. (2011). Transcriptional control of adipose lipid handling by IRF4. Cell Metab. *13*, 249–259.

Enerbäck, S., Jacobsson, A., Simpson, E.M., Guerra, C., Yamashita, H., Harper, M.E., and Kozak, L.P. (1997). Mice lacking mitochondrial uncoupling protein are cold-sensitive but not obese. Nature *387*, 90–94.

Farmer, S.R. (2009). Obesity: be cool, lose weight. Nature *458*, 839–840.

Harms, M.J., Ishibashi, J., Wang, W., Lim, H.W., Goyama, S., Sato, T., Kurokawa, M., Won, K.J., and Seale, P. (2014). Prdm16 is required for the maintenance of brown adipocyte identity and function in adult mice. Cell Metab. *19*, 593–604.

Kang, S., Bajnok, L., Longo, K.A., Petersen, R.K., Hansen, J.B., Kristiansen, K., and MacDougald, O.A. (2005). Effects of Wnt signaling on brown adipocyte differentiation and metabolism mediated by PGC-1alpha. Mol. Cell. Biol. *25*, 1272–1282.

Kong, X., Banks, A., Liu, T., Kazak, L., Rao, R.R., Cohen, P., Wang, X., Yu, S., Lo, J.C., Tseng, Y.H., et al. (2014). IRF4 is a key thermogenic transcriptional partner of PGC-1α. Cell *158*, 69–83.

Laurent, B., Ruitu, L., Murn, J., Hempel, K., Ferrao, R., Xiang, Y., Liu, S., Garcia, B.A., Wu, H., Wu, F., et al. (2015). A specific LSD1/KDM1A isoform regulates neuronal differentiation through H3K9 demethylation. Mol. Cell *57*, 957–970.

Lowell, B.B., S-Susulic, V., Hamann, A., Lawitts, J.A., Himms-Hagen, J., Boyer, B.B., Kozak, L.P., and Flier, J.S. (1993). Development of obesity in transgenic mice after genetic ablation of brown adipose tissue. Nature *366*, 740–742.

Metzger, E., Wissmann, M., Yin, N., Müller, J.M., Schneider, R., Peters, A.H., Günther, T., Buettner, R., and Schüle, R. (2005). LSD1 demethylates repressive histone marks to promote androgen-receptor-dependent transcription. Nature *437*, 436–439.

Musri, M.M., Carmona, M.C., Hanzu, F.A., Kaliman, P., Gomis, R., and Párrizas, M. (2010). Histone demethylase LSD1 regulates adipogenesis. J. Biol. Chem. *285*, 30034–30041.

Ohno, H., Shinoda, K., Ohyama, K., Sharp, L.Z., and Kajimura, S. (2013). EHMT1 controls brown adipose cell fate and thermogenesis through the PRDM16 complex. Nature *504*, 163–167.

Orlicky, D.J., and Schaack, J. (2001). Adenovirus transduction of 3T3-L1 cells. J. Lipid Res. *42*, 460–466.

Seale, P., Bjork, B., Yang, W., Kajimura, S., Chin, S., Kuang, S., Scimè, A., Devarakonda, S., Conroe, H.M., Erdjument-Bromage, H., et al. (2008). PRDM16 controls a brown fat/skeletal muscle switch. Nature *454*, 961–967.

Shi, Y., Lan, F., Matson, C., Mulligan, P., Whetstine, J.R., Cole, P.A., Casero, R.A., and Shi, Y. (2004). Histone demethylation mediated by the nuclear amine oxidase homolog LSD1. Cell *119*, 941–953.

Tallquist, M.D., Weismann, K.E., Hellström, M., and Soriano, P. (2000). Early myotome specification regulates PDGFA expression and axial skeleton development. Development *127*, 5059–5070.

Tharp, K.M., Jha, A.K., Kraiczy, J., Yesian, A., Karateev, G., Sinisi, R., Dubikovskaya, E.A., Healy, K.E., and Stahl, A. (2015). Matrix-assisted transplantation of functional beige adipose tissue. Diabetes *64*, 3713–3724.

van Marken Lichtenbelt, W.D., Vanhommerig, J.W., Smulders, N.M., Drossaerts, J.M., Kemerink, G.J., Bouvy, N.D., Schrauwen, P., and Teule, G.J. (2009). Cold-activated brown adipose tissue in healthy men. N. Engl. J. Med. *360*, 1500–1508.

Virtanen, K.A., Lidell, M.E., Orava, J., Heglind, M., Westergren, R., Niemi, T., Taittonen, M., Laine, J., Savisto, N.J., Enerbäck, S., and Nuutila, P. (2009). Functional brown adipose tissue in healthy adults. N. Engl. J. Med. *360*, 1518–1525.

Wang, J., Scully, K., Zhu, X., Cai, L., Zhang, J., Prefontaine, G.G., Krones, A., Ohgi, K.A., Zhu, P., Garcia-Bassets, I., et al. (2007). Opposing LSD1 complexes function in developmental gene activation and repression programmes. Nature *446*, 882–887.

Wang, L., Xu, S., Lee, J.E., Baldridge, A., Grullon, S., Peng, W., and Ge, K. (2013). Histone H3K9 methyltransferase G9a represses PPARγ expression and adipogenesis. EMBO J. *32*, 45–59.

Wang, J., Telese, F., Tan, Y., Li, W., Jin, C., He, X., Basnet, H., Ma, Q., Merkurjev, D., Zhu, X., et al. (2015). LSD1n is an H4K20 demethylase regulating memory formation via transcriptional elongation control. Nat Neurosci. *18*, 1256–1264.